JPE 17-2-20

https://doi.org/10.6113/JPE.2017.17.2.522
ISSN(Print): 1598-2092 / ISSN(Online): 2093-4718

A Cascaded D-STATCOM Integrated with a Distribution Transformer for Medium-voltage Reactive Power Compensation

Ertao Lei†, Xianggen Yin*, Yu Chen*, and Jinmu Lai *

†,*School of Electrical and Electronic Engineering, Huazhong University of Science and Technology, Wuhan, China

Abstract

This paper presents a novel integrated structure for a cascaded distribution static compensator (D-STATCOM) and distribution transformer for medium-voltage reactive power compensation. The cascaded multilevel converter is connected to a system via a group of special designed taps on the primary windings of the Dyn11 connection distribution transformer. The three-phase winding taps are symmetrically arranged and the connection point voltage can be decreased to half of the line-to-line voltage at most. Thus, the voltage stress for the D-STATCOM is reduced and a compromise between the voltage rating and the current rating can be achieved. The spare capacity of the distribution transformer can also be fully used. The working mechanism is explained in detail and a modified control strategy is proposed for reactive power compensation. Finally, both simulation and scaled-down prototype experimental results are provided to verify the feasibility and effectiveness of the proposed connection structure and control strategy.

Key words: Cascaded multilevel converter, Distribution static compensator (D-STATCOM), Distribution transformer, Reactive power compensation, Winding taps

I. INTRODUCTION

In recent years, distribution static synchronous compensators (D-STATCOMs) have become widely used in low voltage (LV) distribution systems [1], [2]. For high and medium voltage (HV and MV) applications, they are always connected to a grid through a step-down transformer due to the high voltage stresses of the switching devices. As a result, the custom coupling transformer makes the whole system bulky and costly. According to [3] the weight of a prototype D-STATCOM rated at 360-kVA is three tons and the transformer weighs about one ton (nearly one-third of the total weight). In order to reduce volume and weight, modular multilevel cascaded converters (MMCC) have been studied to realize transformer-less D-STATCOM [3]-[6].

The MMCC-based D-STATCOM can realize a high blocking voltage and a low-harmonic output voltage, which makes it possible to eliminate the step-down transformer for medium-voltage (MV) applications. Among the MMCC family members, the single-star bridge cells (SSBC) topology seems to be the most suitable for D-STATCOMs. However, a reasonable compromise between the blocking voltage of the switching devices and the cascaded cells count must be achieved when it is applied to MV distribution systems (with nominal voltages of 10-kV in China, 6.6-kV in Japan or 13.8-kV in the United States). That is to say, if 3.3-kV insulated-gate bipolar transistors (IGBTs) are chosen, the cascaded cell count of per cluster may be four (N=4, taking a 6.6-kV transformer-less D-STATCOM as an example). Meanwhile, if 1.7-kV IGBTs are chosen, the cascaded count is eight (N=8) [7]. More cells in series will reduce the reliability and increase the control complexity. However, fewer cells make it necessary to choose high voltage switching devices. Although various manufactures (Infineon) have announced high power switching devices in ranges from 3.3-kV to 6.5-kV, these HV devices are more expensive and not always available. Their switching frequencies are limited to few hundred hertz [8]. In practice, the 1.7-kV and 1.2-kV IGBTs are the most cost

Manuscript received Aug. 11, 2016; accepted Dec. 3, 2016
Recommended for publication by Associate Editor Il-Yop Chung.
†Corresponding Author: leiertao2008@163.com
Tel: +86-027-87540945, Huazhong University of Science & Technology
*School of Electrical and Electronic Engineering, Huazhong University of Science & Technology, China

effective power switches on the market.

To reduce the voltage stress across the power switch and dc-link capacitor, many hybrid combination structures for passive power filters (PPF) in parallel or series with STATCOMs have been proposed [8]-[11]. These devices are referred as hybrid STATCOMs (H-STATCOMs). Capacitors (C), thyristor switched capacitors (TSCs) or thyristor controlled reactors (TCRs) are connected in series to a voltage source converter (VSC) to indirectly reduce the connection voltage of the STATCOM, since most of the voltage drop occurs on the capacitors or passive branches. These kinds of topologies are helpful for reducing the rating of the dc link voltage of STATCOMs. However, the additional passive components may suffer from a resonance problem. In addition, the coordination control of the passive parts (C, TSC and TCR) and active parts is also a challenge.

Motivated by an autotransformer and considering the actual load characteristics of the existing distribution transformer, an integration structure of a STATCOM and distribution transformer was first proposed in [12], and it was called DT-STATCOM. That paper introduces the multi-group taps structure, and three STATCOMs are located at the vertices of the delta windings.

Unlike previous work, the main contribution of this paper is that a novel three-phase connection type for a CMC-based D-STATCOM and distribution transformer is designed and tested for voltage stress reduction and transformer capacity utilization improvement. The winding-taps (WT) on the primary windings are used for the connection of the VSC instead of the conventional point of common coupling (PCC). The system configuration, compensation mechanism and mathematical model are presented in detail. Considering the amplitude and phase-angle deviations of the voltages and currents between the primary side and the secondary side, a modified decoupled control scheme suitable for the new connection type is proposed. Both simulation and experimental results verify the performance of the proposed connection type for reactive power compensation.

II. System Configuration and Mechanism Analysis

A. Comparisons of Different Connection Points

D-STATCOM systems may be connected to a power grid in different ways for different requirements. The connection points are summarized in Fig. 1(a)-(c) [13], [14]. A D-STATCOM may be installed locally or at the consumer end, as shown in Fig. 1(a). The connection voltage of this configuration is relatively low and the compensation capacity of a single device is limited to several thousand Vars. This connection type is suitable for decentralized compensation. The drawback is that it is very costly and uneconomical to install a D-STATCOM wherever it is required because not all

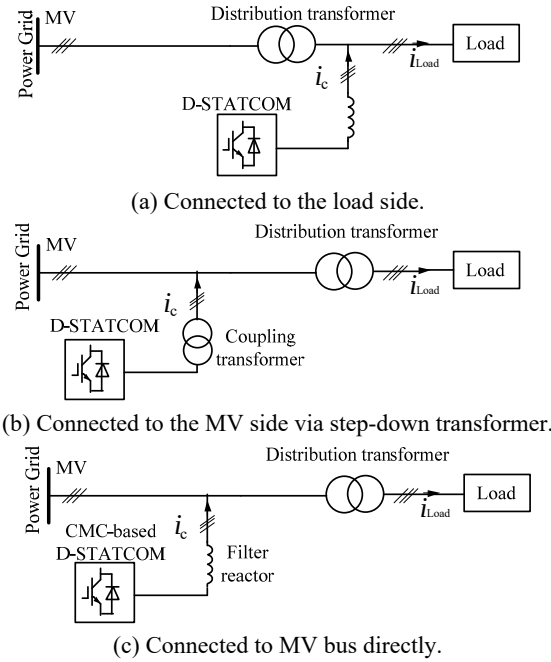

(a) Connected to the load side.

(b) Connected to the MV side via step-down transformer.

(c) Connected to MV bus directly.

Fig. 1. Conventional connection alternatives for D-STATCOM system.

single device can share their compensation capacity with other devices [15]. To reduce the total installed capacity, the centralized configurations are developed as shown in Fig. 1(b) and (c). The compensation capacity of a single device may reach several megavar due to an increased connection voltage. The D-STATCOM is connected to MV buses via the specially designed coupling transformer shown in Fig. 1(b). The rated ac voltage of a CMC is determined by the coupling transformer secondary voltage and it can be chosen among the standard ac voltages specified in the IEC Standard Voltages [16]. As mentioned in Section I, a bulky coupling transformer makes it less attractive than the CMC-based transformer-less D-STATCOM shown in Fig. 1(c). In this case, the rated voltage of the CMC is the line voltage, and this relatively high voltage is handled by a set of cells together in each cluster. The coupling transformer is removed, but the cascaded cell count in series increases, which increases the complexity and unreliability. In addition, the installed capacity is always much greater than the actual demand. That is to say, it is not possible to make full use of the install capacity.

For the three connection types mentioned above, the D-STATCOM and the distribution transformer are considered in isolation. In fact, it is more flexible to use the distribution transformer to realize the changeable connection point voltage for the D-STATCOM. Therefore, the distribution transformer is used as the coupling transformer at the same time in this paper.

B. Proposed Connection Type

In previous research, the actual inductive and capacitive reactive power requirements as well as their daily and monthly

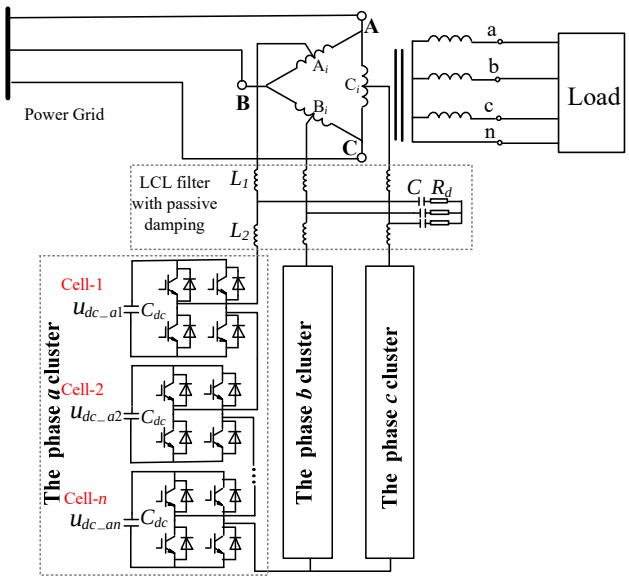

Fig. 2. Proposed connection type for CMC-based D-STATCOM.

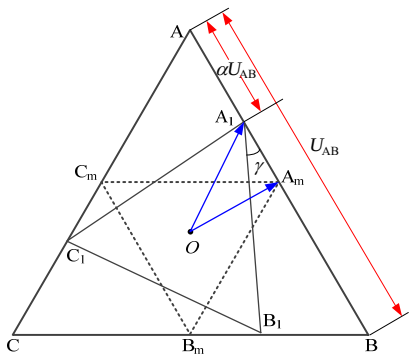

Fig. 3. Connection style of the primary winding with taps.

variation characteristics near the distribution transformer have been studied. The actual load ratio of the existing distribution transformer is always low (below 0.4 most of the time during a day), especially in remote rural areas. When the load ratio of a distribution transformer is relatively low, reactive power takes up a large percent of the apparent power and the power factor (PF) of the source side is usually far below the prescribed value (0.9~0.95). In general, consumers are penalized by power companies for every 0.01 fall in the PF below 0.9. In this case, the PF can be improved more significantly than the high load ratio condition by the D-STATCOM. When the load ratio is relative low, it is possible to make full use of the spare capacity for reactive power compensation.

Fig. 2 shows the proposed connection type for a CMC-based D-STATCOM. A group of winding taps are designed on the primary windings for compensation current injection. To decrease the harmonics injection, a LCL filter with passive damping is configured as the interfacing filter. The connection voltage of the D-STATCOM is U_{AiBi}, U_{BiCi} and U_{CiAi}. When different connection taps are chosen, the connection point voltage is changed.

To clearly explain the changeable connection voltage, two groups of possible winding taps on the primary windings (labeled as A_1-B_1-C_1 and A_m-B_m-C_m) are shown in Fig. 3. To guarantee that the system is working normally, the positions of the taps must be symmetrical, i.e., they must satisfy $|AA_1| = |BB_1| = |CC_1|$. Fig. 3 can also be used to explain the voltage stress the VSC needs to handle. Suppose the voltage of the upper part is αU_{AB} ($0 \le \alpha \le 1$), the line-to-line voltage $U_{A_1B_1}$ can be calculated according to the *law of cosines*:

$$U_{A_1B_1} = U_{AB}\sqrt{3\alpha^2 - 3\alpha + 1}\,. \tag{1}$$

From Equ. (1), it is clear that the minimum connection point (CP) voltage (the line-to-line voltage) is 0.5UAB, and that it is obtained when α=0.5, i.e. the central taps labeled A_m, B_m, and C_m, are chosen as the CP to connect the VSC. Taking the MV distribution network with a nominal line-to-line voltage of 10-kV as an example, the voltage of the compensation current injection point is half of the line voltage, i.e. 5-kV. When different group of taps are chosen, the CP voltage varies from 5-kV to 10-kV.

When applying the proposed connection structure, a compromise between the voltage rating and the current rating of the CMC-based D-STATCOM can be achieved. In addition, the spare capacity of the distribution transformer can be fully used. The D-STATCOM designed for the 6.6-kV distribution system in [4] can be extended to a 10-kV system with a few changes.

C. Compensation Mechanism and Equivalent Circuit

A three-winding autotransformer model is utilized to explain the working mechanism of the proposed connection structure. A single-phase diagram of the proposed connection type is shown in Fig. 4. The subscript symbols “s”, “c” and “t” represent series windings, common windings and tertiary windings, respectively. N_1 is the number of turns of the high voltage (HV) windings, while N_2, and N_3 are medium voltage (MV) windings and low voltage (LV) windings, respectively.

It is important to note the D-STATCOM is controlled as a controlled current source (CCS) in this paper. Therefore, it is modeled as a CCS in Fig. 4.

Apply the reference directions defined in Fig. 4. The induced electromotive force (EMF) equation of the three windings can be expressed as follows:

$$\frac{E_1}{E_c} = \frac{N_1}{N_2} = k_{12}, \quad \frac{E_1}{E_t} = \frac{N_1}{N_3} = k_{13} \tag{2}$$

The EMF of the primary windings is:

$$\dot{E}_1 = -\dot{I}_0 Z_m \tag{3}$$

where Z_m is the magnetizing impedance, and $\dot{I}_0$ is the no-load current. In view of the need for ampere-turns balance, the following is obtained:

$$N_1\dot{I}_1 + N_2\dot{I}_c + N_3\dot{I}_L = N_1\dot{I}_0\,. \tag{4}$$

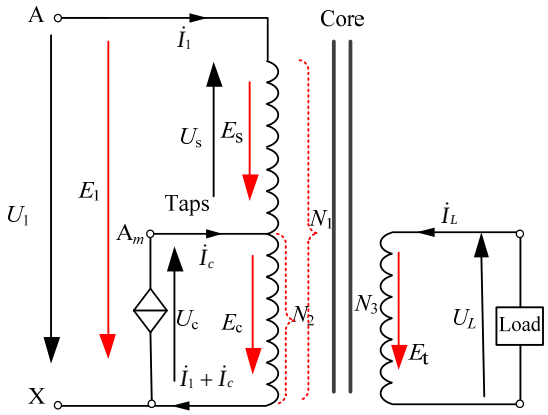

Fig. 4. Single-phase diagram of the proposed WTI D-STATCOM.

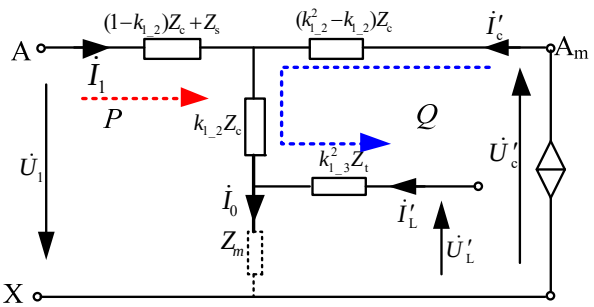

Fig. 5. Equivalent circuit of the proposed structure.

Applying *Kirchhoff's law*, it is possible get equations (5)-(8):

$$\dot{U}_s = \dot{E}_s - \dot{I}_1 Z_s \tag{5}$$

$$\dot{U}_c = \dot{E}_2 - (\dot{I}_1 + \dot{I}_c) Z_c \tag{6}$$

$$\dot{U}_L = \dot{E}_t - \dot{I}_L Z_t \tag{7}$$

$$\dot{U}_1 = -(\dot{U}_c + \dot{U}_s). \tag{8}$$

where Z_s, Z_c and Z_t are the leakage impedance of the series windings, common windings and tertiary windings, respectively. The leakage impedances can be obtained by short circuit tests [17].

In practice, the parameters are usually referred to the primary side (HV side in this case). The combination of Equ. (2) and (8) yields:

$$\dot{U}'_c = k_{12}\dot{U}_c = -\dot{I}_0 Z_m - (\dot{I}_0 - \frac{\dot{I}_L}{k_{13}}) k_{12} Z_c - (k_{12}-1) Z_c \dot{I}_c \tag{9}$$

$$\dot{U}'_L = k_{13}\dot{U}_L = -\dot{I}_0 Z_m - k_{13} Z_t \dot{I}_L \tag{10}$$

$$\dot{U}_1 = \dot{I}_1[(1-k_{12})Z_c + Z_s] + \dot{I}_0 Z_m + (\dot{I}_0 - \frac{\dot{I}_L}{k_{13}}) k_{12} Z_c \tag{11}$$

The equivalent circuit can be obtained from (9) to (11), as shown in Fig. 5. The compensation currents are injected via the taps. If the quantity of the output reactive power of the D-STATCOM is equal to that of the required load, the source only needs to apply active power. In this way, reactive power compensation can be achieved.

III. Control Strategy

The control objectives are as follows. 1) Increasing the capacity utilization of the transformer to ensure its safety. 2) Controlling the CMC-based D-STATCOM to compensate the reactive current completely when the spare capacity of the distribution transformer is permitted. Therefore, the injected current must be well controlled to prevent the transformer from overloading. A control block diagram of the whole system is shown in Fig. 6. It mainly consists of three parts: the injection current calculation, decoupled current control and dc-link voltage control.

A. Injection Current Calculation

The load voltages and currents are detected to calculate the injection currents. The compensation currents are injected through the three-phase winding taps. The current detection point and the injection point are not the same node. There are amplitude and phase-angle deviations between the load currents and the injection currents due to the Dyn11 connection transformer. To clearly explain this, a phasor diagram is given in Fig. 7. The load voltage (secondary voltage) U_a (line-to-neutral) is 30° leading the primary side voltage U_{AO} (Dyn11 connection). If φ is the lagging power factor angle of the load before compensation, then the reactive current component can be expressed as:

$$i_{ql} = I_a \sin\varphi . \tag{12}$$

The D-STATCOM is connected to the winding taps labeled as A_1, B_1 and C_1. Therefore, the rated voltage of the star-configured CMC is U_{A1O}, which can be expressed as (from Fig. 3):

$$U_{A1O} = \sqrt{3\alpha^2 - 3\alpha + 1}\; U_{AO} = \sqrt{3\alpha^2 - 3\alpha + 1}\; kU_a \tag{13}$$

where k is the transformation ratio. Neglecting the active power absorbed by the CMC, the injected reactive current phasor I_{A1} is perpendicular to the connection point voltage U_{A1O}. When the central taps are chosen as the connection taps, I_{A1} is in the same phase or the reversed phase as U_a.

The amplitude of I_{A1} can be calculated by applying the synchronous reference frame (SRF) to the three-phase load current. The phase angle of the load voltages $u_{la,b,c}$ is locked by a phase lock loop (PLL1). Then the reactive component of the load current can be obtained by:

$$\begin{bmatrix} i_{ldref} \\ i_{lqref} \\ i_0 \end{bmatrix} = \frac{2}{3} \begin{bmatrix} \sin\theta & \sin(\theta-120^\circ) & \sin(\theta-120^\circ) \\ \cos\theta & \cos(\theta-120^\circ) & \cos(\theta+120^\circ) \\ 0.5 & 0.5 & 0.5 \end{bmatrix} \begin{bmatrix} i_{la} \\ i_{lb} \\ i_{lc} \end{bmatrix} \tag{14}$$

The reactive component i_{lqref} cannot be used directly. It is transferred to the selective compensation block, which is designed to select complete compensation or partial compensation based on the following criteria:

$$I_{qlref} = \begin{cases} I_{qlref}, & if\ \beta \le \beta_0 \\ \lambda I_{qlref}, & if\ \beta > \beta_0 \end{cases} \tag{15}$$

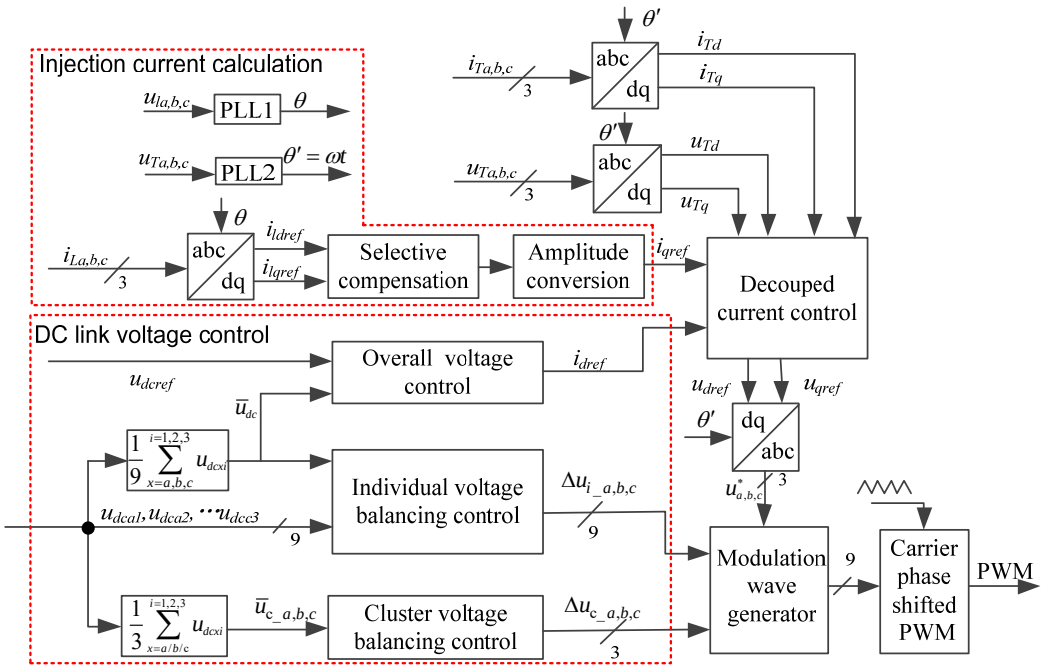

Fig. 6. Control block diagram of the prototype system.

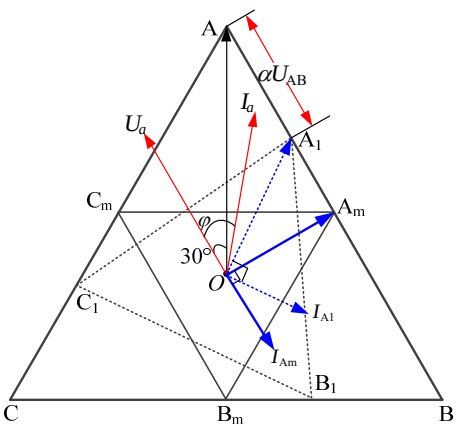

Fig. 7. Phasor diagram of the voltages and current across the transformer.

In (15), β is the actual load ratio of the distribution transformer, β_0 is the maximum allowable load ratio, and λ is the compensation coefficient ($0<\lambda<1$). The actual load ratio can be calculated via:

$$\beta=\frac{\sqrt{I_1^2+I_2^2+\cdots I_n^2}+i_{eq}}{I_N} \tag{16}$$

where I_1, I_2,…I_n are the RMS values of the fundamental, second harmonic,…nth harmonic components of the load currents (converted to the primary side), respectively; and I_N is the rated current of the transformer on the primary side. i_{eq} is the approximate equivalent current, which represents the losses (including no-load losses and load losses) of the distribution transformer itself. Generally, it is not easy to accurately measure the total losses of the transformer, because the load losses are variable under different load conditions. Thus, the corresponding equivalent current i_{eq} cannot be obtained easily. Considering that these losses are only a small part of the power rating of the transformer (usually less than 5%), i_{eq} is set to 0.05 I_N to simplify the calculation.

The maximum allowable load ratio β_0 is determined by the rated current of the primary windings. To prevent the windings from overcurrent after current injection, the following constraint must be satisfied:

$$\max\{i_{AAm}, i_{AmX}\}\le I_N \tag{17}$$

where i_{AAm} and i_{AmX} are the currents of the series winding and the common winding in phase a, respectively. In general, it is not easy to directly measure the winding currents. From Fig. 4, the proposed connection type is similar to an autotransformer. According to autotransformer theory, the capacities of the series winding and the common winding are equal, i.e. $S_{AAm}=S_{AmX}$. Assuming that the apparent power of a two-winding transformer is S_N, it is possible to obtain:

$$S_{AAm}=S_{AmX}=S_N\left(1-\frac{1}{K_A}\right) \tag{18}$$

where K_A is the voltage ratio and $K_A=N_1/N_2$. In this paper, the central taps are chosen as the connection points. Thus, it is possible to obtain $K_A=2$ and $S_{AAm}=S_{AmX}=0.5S_N$. Considering the safety margin, the maximum allowable load ratio β_0 is set as 0.4 according to field tests, and verified by experiments.

If the actual load ratio is less than β_0, the reactive current is completely compensated. Meanwhile, if β is greater than β_0, complete compensation may cause an overcurrent of the transformer windings (shown in the Appendix).

The output of the selective compensation block should be converted to the current injection point based on the reactive power balance principle by the amplitude conversion block. This can be expressed as:

$$I_{qref} = \frac{I_{lqref} \cdot U_a}{U_{A1O}} = \frac{I_{lqref}}{k\sqrt{3\alpha^2 - 3\alpha + 1}}. \quad (19)$$

B. Decoupled Current Control

Conventional PI controllers are applied for inner loop current control. The difference is that the connection point of the D-STATCOM is the winding taps instead of the PCC. The phase angle θ' of the taps voltages (subscript *T*) is locked by PLL2. The *d*-axis and *q*-axis components of u_{Tabc} and i_{Tabc} can be obtained by applying a *d-q* transformation. The controller can be designed as:

$$\frac{d}{dt}\begin{bmatrix} i_{Td} \\ i_{Tq} \end{bmatrix} = L\begin{bmatrix} K_p(i_{dref} - i_{Td}) + K_i\int(i_{dref} - i_{Td})dt \\ K_p(i_{qref} - i_{Tq}) + K_i\int(i_{qref} - i_{Tq})dt \end{bmatrix} \quad (20)$$

where $L=L_1+L_2$ is the equivalent inductance of the LCL filter, and K_p and K_i are the proportional gain and integral gain, respectively.

C. DC Link Voltage Balancing Control

For the CMC-based transformer-less D-STATCOM, it is essential to balance the dc capacitor voltage. Many dc capacitor voltage balancing control methods have been presented for the CMC-based STATCOM [18], [19]. The voltage balancing control method proposed in [6] and [19] is applied here. This voltage balance control consists of three layers: overall voltage control, cluster voltage balancing control (CVBC) and individual voltage balancing control (IVBC). In Fig. 2, the reference dc link voltage of each cell is u_{dcref}. The dc capacitor voltage of each cell is u_{dc_xi} $(x=a,b,c;i=1,2,\cdots n)$. The dc mean voltage of all of the cells is given by:

$$\overline{u}_{dc} = \frac{1}{3n}\sum_{x=a}^{c}\sum_{i=1}^{n} u_{dc\_xi}. \quad (21)$$

The dc mean voltage of one cluster is given by:

$$\overline{u}_{dc\_x} = \frac{1}{n}\sum_{i=1}^{n} u_{dc\_xi} (x = a,b,c). \quad (22)$$

The overall voltage balancing control is designed to achieve $\overline{u}_{dc}$ approaching u_{dcref} ($\overline{u}_{dc} \to u_{dcref}$). The cluster CVBC is designed to achieve $\overline{u}_{dc\_x}$ approaching $\overline{u}_{dc}$ ($\overline{u}_{dc\_x} \to \overline{u}_{dc}$), while the IVBC is designed to achieve u_{dc_xi} approaching $\overline{u}_{dc\_x}$ ($u_{dc\_xi} \to \overline{u}_{dc\_x}$).

The overall voltage control considers a set of three clusters as a three-phase full-bridge converter using six IGBTs. This can be achieved by adjusting the *d*-axis current command i_{dref}. The controller can be expressed as:

$$i_{dref} = K_{p\_udc}(u_{dcref} - \overline{u}_{dc}) + K_{i\_udc}\int(u_{dcref} - \overline{u}_{dc})dt \quad (23)$$

where K_{p_udc} and K_{i_udc} are the proportional and integral gain, respectively.

A similar method, presented in [19], is applied for the CVBC and the IVBC. A visualized explanation for the *a*-phase *i*th cell is shown in Fig. 8. The idea is that two voltage vectors u_{c_a} and u_{m_ai} are added to the reference voltage u_{aref} to produce a minor pulse width adjustment. This adjustment can change the active power absorbed by the H-bridge cell. The procedures for designing appropriate voltage vectors are given in the following part.

The minor voltage vector u_{c_x} for the CVBC (being in phase or out of phase by 180° with the ac output signal u_{xref} from the decoupled current control) is superimposed to the output voltage of each cluster. The voltage vectors can be designed as:

$$\begin{bmatrix} u_{c\_a} \\ u_{c\_b} \\ u_{c\_c} \end{bmatrix} = K_c S\begin{bmatrix} \overline{u}_{dc} - \overline{u}_{dc\_a} \\ \overline{u}_{dc} - \overline{u}_{dc\_b} \\ \overline{u}_{dc} - \overline{u}_{dc\_c} \end{bmatrix} \quad (24)$$

where K_c is the proportional gain and the matrix $S=diag\{\sin\theta', \sin(\theta'-120^\circ), \sin(\theta'+120^\circ)\}$. Detailed step-by-step procedures for designing the gain parameters are given in [19]. The control block diagram is redrawn in Fig. 9.

The voltage vector of the *a*-phase is given by:

$$u_{c\_a} = K_3[K_2(\overline{u}_{dc} - \overline{u}_{dc\_a}) - i_d]\sin(\omega t) \quad (25)$$

In the steady state, the dc mean voltage for all of the cells $\overline{u}_{dc}$ is very close to its reference value u_{dcref} (it has a margin of error of plus or minus 2 percent). Therefore, the output of the outer-loop PI controller (i_{dref}) is relatively small according to equation (23). The active current component i_d in (25) should track the *d*-axis current reference i_{dref} obtained from (23). Generally, the response speed of the inner current loop is much faster than that of the outer voltage loop. As a result, i_d tracks i_{dref} in a short time. Hence, i_d is relatively small in the steady state (only balancing the power losses of the converter).

On the other hand, the CVBC is the second layer dc-link voltage balancing control. It is realized on the foundation of the overall voltage control (first layer). The system can be regarded as being approximately in the steady state when designing the CVBC. Therefore, the active current component i_d in (25) can be neglected. Finally, the superposed voltage vector for the CVBC can be expressed as:

$$u_{c\_a} = K_3[K_2(\overline{u}_{dc} - \overline{u}_{dc\_a})]\sin(\omega t) \quad (26)$$

Therefore, the gain K_c is set to K_2K_3 in the proposed design. To select appropriate values for K_2 and K_3, the inner-loop transfer function ***G*** according to Fig. 9 is written as:

$$G = \frac{K_3K_{PWM}}{sL_{AC} + K_3K_{PWM}} \quad (27)$$

The converter gain $K_{PWM} = 1$, is a first-order system with a time constant of:

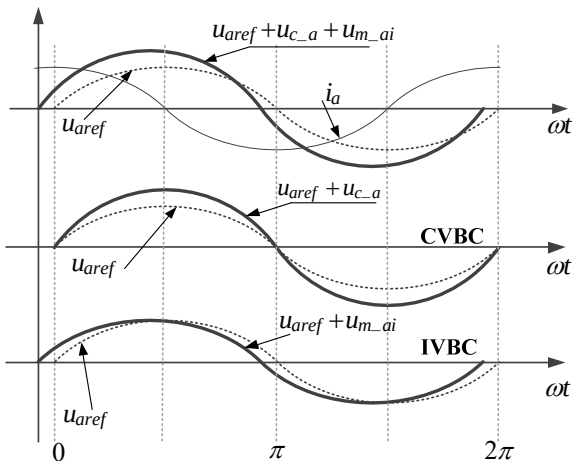

Fig. 8. Visualized explanation of the CVBS and IVBS for *a*-phase *i*th cell.

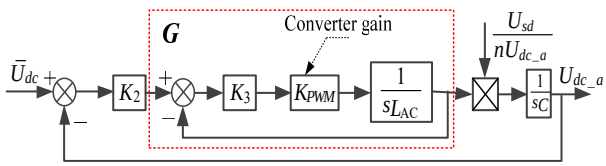

Fig. 9. Control block diagram of the CVBS for *a*-phase.

$$\tau_c = \frac{L_{AC}}{K_3 K_{PWM}} \approx \frac{L_{AC}}{K_3} \tag{28}$$

In general, the time constant is set to a fundamental period ($\tau_c = 20ms$), so the first parameter K_3 can be obtained from $K_3 = L_{AC}/\tau_c$. Similarly, the overall transfer function can be expressed as:

$$\frac{U_{dc}}{\bar{U}_{dc}} = \frac{K_2 K_3 U_{sd}}{(CL_{AC} nU_{dc\_a})s^2 + (CK_3 nU_{dc\_a})s + K_2 K_3 U_{sd}} \tag{29}$$

It is a typical second-order system and the damping ratio is given by:

$$\zeta = \frac{1}{2}\sqrt{\frac{nCK_3 U_{dc\_a}}{K_2 U_{sd} L_{AC}}} \tag{30}$$

According to control theory, ζ is selected as the optimal damping ratio, i. e. $\zeta = 0.707$. Then it is possible to obtain an appropriate K_3 from (30).

Taking phase *a* as an example to explain the IVBC, the D-STATCOM mainly draws reactive power from the grid in the steady state ($i_{Tq} \gg i_{Td}$). Therefore, the current flowing in phase *a* can be expressed as:

$$i_a = I_q \cos(\omega t) \tag{31}$$

To produce an amount of active power for each capacitor voltage balancing, the idea is superimposing a voltage vector in the same phase or reversed phase as i_a to the reference voltage of the corresponding cell. Therefore, it is possible to design the following voltage vector as:

$$\begin{aligned} u_{m\_ai} &= K_{i\_udc}(\bar{u}_{dca} - u_{dc\_ai})\cos(\omega t) \\ &= K_{i\_udc}\Delta u_{dc\_ai}\cos(\omega t) \end{aligned} \tag{32}$$

The sign of the gain K_{i_udc} depends on the operation mode of the D-STATCOM. It is positive for the inductive mode and negative for the capacitive mode. The controller gain K_{i_udc} is designed considering two aspects. One is the operation range of the D-STATCOM, and the other is the response speed.

1) Operation Range. As mentioned above, the active power for the IVBC is influenced by the *q*-axis current command i_{qref} (reactive current command). This means that the IVBC dose not work when $i_{qref} = 0$. The produced active power is different for different values of i_{qref} corresponding to different operation conditions under the same controller gain K_{i_udc} . If the D-STATCOM is working close to its rated capacity (i_{qref} is close to its upper limit $i_{\max}$), too large a gain may cause instability. Therefore, a tradeoff is made to adapt to different values of i_{qref} and it is assumed that the D-STATCOM is working under the half load condition ($i_{qref} = \pm 0.5 i_{q\max}$) to design the gain.

2) Response Speed. The IVBC is designed to be slower in response speed than the cluster balancing control to avoid a conflict of control between the two. This has been verified in [6] by experimental results. Therefore, the IVBC is regarded as a voltage controller in the proposed design. A detailed derivation is given as follows:

The active power for the dc-voltage of the *a*-phase *i*th cell can be obtain from equations (31) and (32):

$$P_{ai} = u_{dcai} \cdot i_{dcai} = (\bar{u}_{dca} - \Delta u_{dcai}) \cdot C \frac{d(\bar{u}_{dca} - \Delta u_{dcai})}{dt} \tag{33}$$

As mentioned above, the IVBC is slower in response time than the cluster balancing control. Therefore, the dc mean voltage $\bar{u}_{c\_a}$ in (33) can be regarded as a constant. Considering $\bar{u}_{c\_a} \gg \Delta u_{dcai}$, (33) can be expressed as:

$$P_{ai} = -C\bar{u}_{dca} \frac{d\Delta u_{dcai}}{dt} \tag{34}$$

From equation (31)-(34), the control block diagram of the IVBC can be obtained, as shown in Fig. 10.

The closed loop transfer function is given by:

$$\frac{\Delta U_{dcai}(s)}{D_{ai}(s)} = \frac{1}{sC\bar{U}_{dca} + K_{i\_udc} I_q} \tag{35}$$

The time constant of the transfer function is given by:

$$\tau = \frac{C\bar{U}_{dca}}{K_{i\_udc} I_q} \tag{36}$$

The time constant can be chosen according to on-site tuning as long as it can guarantee that the respond speed is slower than the cluster balancing control (in [6], it was set to 5s). Once the time constant is determined ($\tau = \tau_0$), the controller gain K_{i_udc} can also be determined form (36), i. e.:

$$K_{i\_udc} = \frac{C\bar{U}_{dca}}{\tau_0 I_q} \tag{37}$$

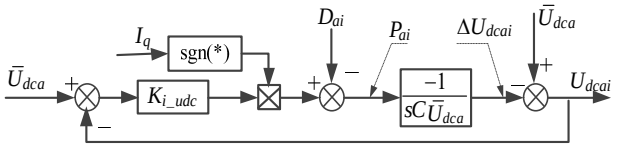

Fig. 10. Control block diagram of the IVBC for *a*-phase *i*th cell.

Consider the operation range mentioned above, I_q is set to $0.5I_{q\max}$ as a compromise.

IV. Simulation Analysis and Experimental Verification

A. Simulation Analysis

To verify the feasibility and effectiveness of the proposed connection type and its performance, simulations are performed in the Matlab/Simulink environment. The specially designed multi-taps distribution transformer is modeled by three single phase multi-winding transformers provided by SimPowerSystem. To simplify the verification, a 9-level CMC-based D-STATCOM with a LCL filter is connected to the central taps of the distribution transformer for compensation currents injection. The simulation parameters are listed in Table I.

At first, the load is set to 200kW+*j*200kVar (inductive). The load ratio of the transformer is about 0.3. Fig. 11 (a)-(d) shows simulation results when the STATCOM is working in the inductive mode. At *t*=0.1s, the STATCOM is switched on. An orthogonal compensation current (u_{TA} is leading i_{TA} by 90 degrees) is injected via the winding taps. After compensation, the source current is completely in phase with the source voltage in less than half of a power cycle. Meanwhile, the source current is significantly reduced. The connection point voltage of the D-STATCOM is only half of the line voltage.

To test the dynamic performance of the proposed structure, a sudden load change form inductive to capacitive (-*j*200kVar) is made at *t*=0.2s. Fig. 12 (a) and (b) show simulation results in this case. When the load is changed, the source current is always in phase with the source voltage. However, the phase of the injection current changes from lagging to leading. It can also be observed that the D-STATCOM obtains a good dynamic compensation performance. The response time is less than half of a fundamental cycle.

B. Experimental Verification

To further validate the proposed connection type, a down-scaled experimental prototype is developed in the laboratory. The prototype comprises a specially designed dry-type transformer with a rated capacity of 50-kVA and a CMC-based 7-level converter. The transformer is shown in Fig. 13. Each phase has five winding taps labeled X_1 to X_5 (X=A, B and C) on the primary windings. The position of the phase-A taps is shown on the left of Fig. 13. The rated voltage of the primary winding is 800V. A_3 is a central tap and the voltage is

TABLE I
Simulation Parameters

Parameter	Value
Source voltage	10kV rms line to line, 50Hz
Distribution transformer	1MVA, 10kV/380V, Dyn11
Switching frequency	2-kHz
LCL filter	L_1=2mH, L_2=0.6mH,C=15 μF, R_d=5 Ω
DC link capacitor	C_{dc}=6000 μF
DC link voltage	1500V

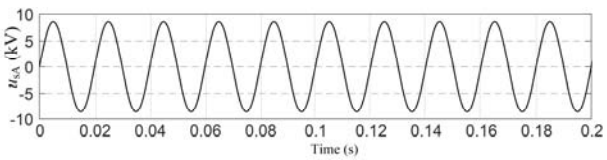

(a) Source voltage u_{sA} (line-to-neutral).

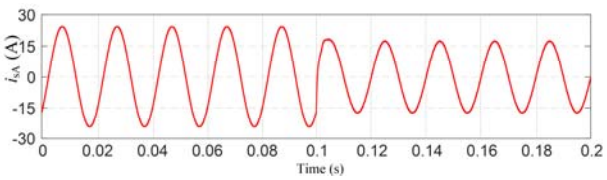

(b) Source current i_{sA}.

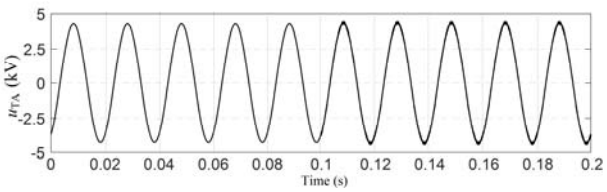

(c) Connection point voltage u_{TA}.

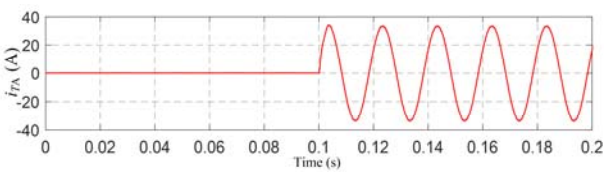

(d) Injection current i_{TA}.

Fig. 11. Simulation results of proposed structure working in inductive mode.

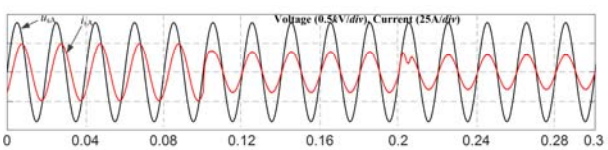

(a) Source voltage and current.

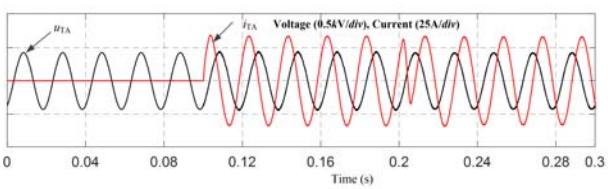

(b) Connection point voltage and injection current.

Fig. 12. Simulation results in a transient state from inductive operation to capacitive operation.

TABLE II
PARAMETERS OF THE EXPERIMENTAL SYSTEM

Parameters	Value
Source voltage	800V,rms line-to-line, 50Hz
System impedance*	12 Ω
Distribution transformer	50kVA, 800/380V, Dyn11
Switching frequency	2kHz
LCL filter	L_1=1mH, L_2=0.2mH, C=10 μF, R_d=2 Ω
Maximum output current of APF	25A (Amplitude)
Cascaded count	3

*Large system impedance is employed according to the safety codes of the authors' lab.

Fig. 13. Image of the three-phase transformer with several taps.

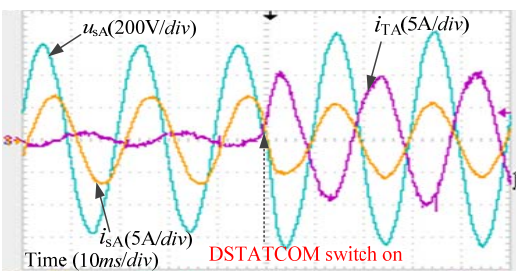

Fig. 14. Experimental waveforms show dynamic performance of the proposed structure.

400V. The other taps are placed symmetrically. To simulate a reactive load, an active power filter (APF) with a rated current of 25A is adopted to generate reactive power and it is configured in parallel with the active load. The other parameters are shown in Table II.

At first, the active load is set to 4.8-kW and the APF is controlled to generate a 10A (amplitude) reactive current to simulate a 4.6-kVar reactive load (inductive). Therefore, the power factor (PF) of the load side can be easily calculated as 0.72. The actual load ratio of the transformer is about 0.15.

Fig. 14 shows experimental results and u_{sA}, i_{sA} and i_{TA} are the source voltage (line-to-neutral), source current and injection current of phase-A, respectively. When the D-STATCOM is switched on, the compensation current i_{TA} is injected through the winding taps. The voltage and current of

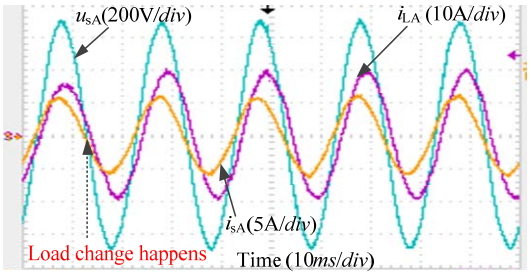

(a) Source voltage u_{sA}, source current i_{sA} and load current i_{LA}.

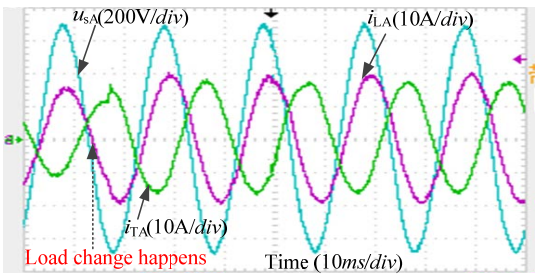

(b) Injected current i_{TA}.

Fig. 15. Experimental results under load sudden change.

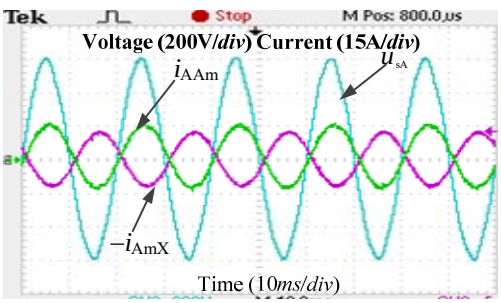

(a) Before compensation.

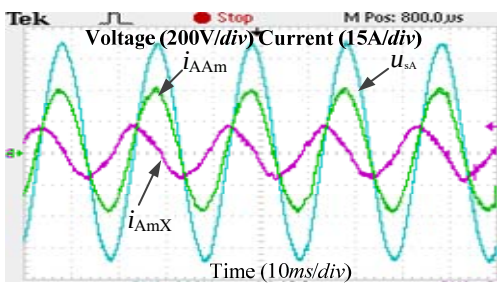

(b) After complete compensation.

Fig. 16. Waveforms of the winding currents in phase *a* under inductive operation mode.

the 800V source are almost in phase with each other after about half of a power cycle (10*ms*). The PF of the source side is increased to unity power factor.

The reactive current is compensated effectively with the winding taps injection method. From Fig. 14, it can be seen that the primary side voltage of the distribution transformer is also increased due to the reduced line drop.

In the following test, the initial reactive current generated by the APF is set to 10A (amplitude, capacitive) and increased to 15A suddenly to simulate the sudden load change condition. The load ratio of the transformer is

increased to 0.23.

The selective compensation and amplitude conversion blocks shown in Fig. 10 are designed to prevent the transformer form overloading after compensation current injection. The threshold value of β_0 is set to 0.2, i.e. if the actual load ratio of the distribution transformer is greater than 0.2, the actual injection currents are limited to its upper limit. In this case, the reactive current is not compensated completely. The source voltage u_{sA} and current i_{sA} are not exactly in phase, as shown in Fig. 15(a). Once a load change occurs (the load current of phase-A i_{LA} increases), the D-STATCOM can increases and inject its output current via the winding taps in less than 10*ms*, as shown in Fig. 15(a) and (b). The PF is increased from 0.38 to 0.9. The results demonstrate the effectiveness of the proposed connection type for reactive power compensation.

V. CONCLUSIONS

In this paper, a novel connection type for the D-STATCOM and distribution transformer is proposed for medium voltage reactive power compensation. The VSC is connected to the three-phase symmetrical winding taps on the primary windings of the transformer for compensation current injection. This way the distribution transformer is used as a coupling transformer of the CMC-based D-STATCOM. The spare capacity of the transformer can be fully used. Both simulation and experimental test results validate the effectiveness of the winding taps injection method.

APPENDIX

The maximum allowable load ratio β_0 is tested in the lab. Fig. 16 shows waveforms of the winding currents before and after compensation. The currents are measured by *Tek*-A622 current probes. Before compensation, the load ratio is set to 0.45 and the currents of the two winding segments AAm and AmX are almost the same (Note that i_{AmX} is in the reverse phase to show the two curves clearly), as shown in Fig. 16(a). After complete compensation, the currents of the two segments are not equal and i_{AAm} is greater than i_{AmX}, which is similar to the operation characteristic of the autotransformer. The load ratio is greater than β_0 (0.4) and i_{AAm} is close to the rated current of the windings (30A), which verifies the analysis in section III-A.

ACKNOWLEDGMENT

This study was supported by the National Natural Science of China under Grant 51277084.

REFERENCES

[1] F. Shahnia, S. Rajakaruna, and A. Ghosh, *Static Compensators (STATCOMS) in Power Systems*, Springer, 2015.

[2] O. P. Mahela and A. G. Shaik, "A review of distribution static compensator," *Renewable and Sustainable Energy Reviews*, Vol. 50, pp. 531-546, Oct. 2015.

[3] K. Sano and M. Takasaki, "A Transformerless D-STATCOM based on a multivoltage cascade converter requiring no dc sources," *IEEE Trans. Power Electron.*, Vol. 27, No. 6, pp. 2783-2795, Mar. 2012.

[4] H. Akagi, H. Fujita, S. Yonetani, and Y. Kondo, "A 6.6-kV transformerless STATCOM based on a five-level diode-clamped PWM converter: System design and experimentation of a 200-V 10-kVar laboratory model," *IEEE Trans. Ind. Appl.*, Vol.44, No.2, pp. 672-680, Mar. 2008.

[5] H. P. Mohammadi and M. T. Bina, "A transformerless medium-voltage STATCOM topology based on extended modular multilevel converters," *IEEE Trans. Power Electron.*, Vol.26, No.5, pp. 1534-1545, May 2011.

[6] H. Akagi, S. Inoue, and T. Yoshii, "Control and performance of a transformerless cascade PWM STATCOM with star configuration," *IEEE Trans. Ind. Appl.*, Vol.43, No.4, pp. 1041-1049, Jun. 2007.

[7] J. I. Y. Ota , Y. Shibano, N. Niimura, and H. Akagi, "A phase-shifted-pwm D-STATCOM using a modular multilevel cascade converter (SSBC)-part I: modeling, analysis, and design of current control," *IEEE Trans. Ind. Appl.*, Vol.51, No.1, pp. 279-288, Jan. 2015.

[8] M. K. Sahu and G. Poddar, "Transformerless hybrid topology for medium-voltage reactive-power compensation," *IEEE Trans. Power Electron.*, Vol. 26, No. 5, pp. 1469-1479, Jun. 2011.

[9] L. Wang, C. S. Lam, and M. C. Wong, "A hybrid-STATCOM with wide compensation range and low DC-Link voltage," *IEEE Trans. Ind. Electron.*, Vol. 63, No. 6, pp. 3333-3343, Jun. 2016.

[10] S. Rahmani, A. Hamadi, K. Al-Haddad, and L. A. Dessaint, "A combination of shunt hybrid power filter and thyristor-controlled reactor for power quality," *IEEE Trans. Ind. Electron.*, Vol.61, No.5, pp. 2152-2164, Oct. 2014.

[11] C. Kumar and M. K. Mishra, "An improved hybrid DSTATCOM topology to compensate reactive and nonlinear loads," *IEEE Trans. Ind. Electron.*, Vol. 61, No. 12, pp. 6517-6527, Dec. 2014.

[12] C. Wang, X. Yin, Z. Zhang, and M. Wen, "A novel compensation technology of static synchronous compensator integrated with distribution transformer," *IEEE Trans. Power Del.*, Vol. 28, No. 2, pp. 1032-1039, Apr. 2013.

[13] B. Gultekin and M. Ermis, "Cascaded multilevel converter-based transmission STATCOM: system design methodology and development of a 12 kV ±12 Mvar power stage," *IEEE Trans. Power Electron.*, Vol. 28, No. 11, pp. 4930-4950, Nov. 2013.

[14] C. O. Gercek and M. Ermis, "Elimination of coupling transformer core saturation in cascaded multilevel converter-based T-STATCOM systems," *IEEE Trans. Power Electron.*, Vol. 29, No. 12, pp. 6796-6809, Dec. 2014.

[15] S. X. Chen, Y. S. Foo. Eddy, H. B. Gooi, M. Q. Wang, and S. F. Lu, "A centralized reactive power compensation system for LV distribution networks," *IEEE Trans. Power Syst.*, Vol. 30, No. 1, pp. 274-284, Jan. 2015.

[16] IEC Standard Voltages, IEC 60038, Edition 7.0, 2009-06.

[17] A. C. Franklin and D. P. Franklin, "*The J & P Transformer Book: A Practical Technology of the Power*

Transformer," Elsevier, 2013.
[18] Z. Liu, B. Liu, S. Duan, and Y. Kang, "A novel dc capacitor voltage balance control method for cascade multilevel STATCOM," *IEEE Trans. Power Electron.*, Vol. 27, No. 1, pp. 14-27, Jan. 2012.
[19] L. Maharjan, S. Inoue, and H. Akagi, "A transformerless energy storage system based on a cascade multilevel PWM converter with star configuration," *IEEE Trans. Ind. Appl.*, Vol.44, No.5, pp. 1621-1630, Sep./Oct. 2008.

Ertao Lei was born in Henan, China. He received his B.S. degree in Electrical Engineering from the Harbin Institute of Technology (HIT), Harbin, China, in 2012. He is presently working towards his Ph.D. degree at the Huazhong University of Science and Technology (HUST), Wuhan, China. His current research interests include reactive power control, power quality, and the application of power electronics in power systems.

Xianggen Yin received his Ph.D. degree in Electrical Engineering from the Huazhong University of Science and Technology (HUST), Wuhan, China, in 1989. Since 1994, he has been a Professor in the School of Electrical and Electronic Engineering, HUST. His current research interests include protective relaying, power system stability control, and the application of power electronics in power systems.

Yu Chen was born in Henan, China, in 1990. He received his B.S. degree from the College of Electrical and Information Engineering, Hunan University, Changsha, China, in 2013. He is presently working towards his Ph.D. degree at the Huazhong University of Science and Technology (HUST), Wuhan, China. His current research interests include the modeling and control of power converters.

Jinmu Lai was born in Fujian, China, in 1990. He received his B.S. degree from the School of Electrical and Electronic Engineering of the Huazhong University of Science and Technology (HUST), Wuhan, China, in 2014, where he is presently working towards his M.S. degree. His current research interests include the modeling and control of power converters and renewable energy generation systems.